Philosophical Magazine A, 1979, Vol. 40, No. 4, 497–510

18

Direct TEM determination of intrinsic and extrinsic stacking fault energies of silicon

By H. Föll† and C. B. Carter
Department of Materials Science and Engineering,
Cornell University, Ithaca, New York 14853, U.S.A.

[Received 12 October 1978 and accepted 5 May 1979]

Abstract

The intrinsic and extrinsic stacking fault energies of silicon have been determined from images of double ribbons obtained using the weak-beam method of electron microscopy. The ribbons occurred in distorted regions of small-angle twist boundaries on {111} planes prepared by welding. The results are compared with values obtained from isolated dislocations in the screw and edge orientation in the same sample, which were found to be consistently lower than the values obtained from double ribbons. It is found that, contrary to other recent work, the ratio $\gamma_{in}:\gamma_{ex}$ is actually only $\sim 14\%$ greater than unity.

§ 1. Introduction

A comprehensive understanding of the properties of dislocations and related defects (such as stacking faults and grain boundaries) ultimately demands a detailed knowledge of their core structure. This is true both for mechanical properties such as dislocation mobilities (see, for example, Wessel and Alexander 1977) and for electronic properties (see, for example, Labusch and Schröter 1975). However, despite extensive recent work, even the basic question concerning dislocations in a diamond-type lattice, namely whether they are of the 'glide set' or 'shuffle set' geometry (Wessel and Alexander 1977, Hirth and Lothe 1968, Blanc 1975), is not yet resolved. The dissociation of either of these configurations is possible (albeit unlikely in the shuffle set) and dissociated defects have been shown to exist in Si and Ge. The first observations were made on extended dislocation nodes by Aerts, Delavignette, Siems and Amelinckx (1962), using conventional strong-beam imaging conditions and were subsequently shown to be inconclusive (Booker and Brown 1965) because of possible contrast artifacts ; some doubt remained whether or not dislocations in Si and Ge were dissociated at all (Haasen and Schröter 1970). This question was unambiguously resolved by Ray and Cockayne (1971) who, using the weak-beam technique, directly observed dislocations split into partials in Si. Subsequently similar observations were made in Ge (Ray and Cockayne 1973, Häussermann and Schaumburg 1973). Values for the intrinsic stacking fault energy, γ_{in}, derived in these studies were $\gamma_{in}=51$ mJ m^{-2} for Si and $\gamma_{in}=60$ mJ m^{-2} for Ge. The extrinsic stacking fault energy γ_{ex} in Si was estimated

† Present address : IBM Research Center, P.O. Box 218, Yorktown Heights, New York 10598, U.S.A.

to be " of the same order of magnitude " because extrinsic nodes were observed to be similar in size to intrinsic nodes (Ray and Cockayne 1971).

More recently, Gomez, Cockayne, Hirsch and Vitek (1975) investigated the dissociation of dislocations close to a screw orientation in Ge and, to a lesser extent, in Si. These authors observed near-screw dislocations having two distinctly different dissociation widths and found that the dislocations with a larger dissociation width contained an extrinsic stacking fault. They concluded that the value of the extrinsic stacking fault energy in Ge and Si is approximately half that of the intrinsic one.

A recent study on Ge (Packeiser and Haasen 1977) confirmed that two different dissociation widths, differing by a factor of 2, appeared to exist for the screw dislocation, but it did not identify the nature of the stacking fault. It has also been recently shown (Wessel and Alexander 1977) that although greatly different dissociation widths could be found for dislocations of the same character in silicon, this was associated with the properties of the partial dislocations rather than the existence of an extrinsic stacking fault. Observations on double ribbons (also known as fault pairs), reported here for the first time in a material with the diamond cubic structure, allow the ratio $\gamma_{\mathrm{in}} : \gamma_{\mathrm{ex}}$ for silicon to be determined directly on a single defect. Because of the large width of the defect it is expected that any core effects, which might otherwise make continuum elasticity theory inapplicable, will be smaller than for single dissociated dislocations and that the numerical values for $\gamma_{\mathrm{in,\,ex}}$ will be closer to those associated with infinite stacking faults.

§ 2. Geometry and theory of double ribbons

Double ribbons were first observed in layer compounds (see, for example, Delavignette and Amelinckx 1961) and subsequently in low stacking fault energy f.c.c. (Gallagher 1966) and h.c.p. (Ruff and Ives 1969) alloys. This is, however, the first observation of such defects in a relatively high-stacking-fault-energy material or one with the diamond-cubic lattice.

Figure 1 shows the geometry of a double ribbon formed by a disturbance of an otherwise regular dislocation network (fig. 1 (*a*)) and the corresponding cross-section (fig. 1 (*b*)). The main properties of double ribbons are as follows.

(1) The three partial dislocations forming the double ribbon have identical Burgers vectors. Residual stresses in the specimen thus will not change its width but only translate the configuration as a whole (in contrast to single dislocations—see Wessel and Alexander (1977)).

(2) Using isotropic elasticity theory, the stacking fault energies $\gamma_{\mathrm{in,\,ex}}$ are related to the respective dissociation widths $r_{\mathrm{in,\,ex}}$ (see fig. 1) by (Gallagher 1966) :

$$\gamma_{\mathrm{in,\,ex}} = \frac{\mu b^2}{2\pi(1-\nu)}\left([1-\nu]\cos^2\beta + \sin^2\beta\right)\left(\frac{1}{r_{\mathrm{in,\,ex}}} + \frac{1}{r_{\mathrm{in}} + r_{\mathrm{ex}}}\right), \qquad (1)$$

where b is the magnitude of the Burgers vector, μ the shear modulus, ν Poisson's ratio and β the angle between line direction and the Burgers vector. On evaluating this formula for a given value of $\gamma_{\mathrm{in,\,ex}}$, it is found that $r_{\mathrm{in,\,ex}}$ are considerably larger than the dissociation width

Fig. 1

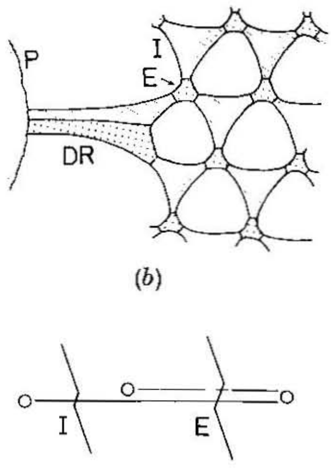

(*b*)

(*a*)

(*a*) Schematic drawing of a dislocation network with extended intrinsic (I) and extrinsic (E) nodes forming a double ribbon at an amorphous precipitate (P). The nodes and the double ribbon are all in the screw orientation. (*b*) Cross-section through a double ribbon on (111). Note that the outer screw dislocation bounding the extrinsic fault may be considered to consist of two 60° dislocations on adjacent glide planes. The dislocations are represented by circles and the inclined lines may represent $(11\bar{1})$ planes.

of single dislocations and thus can be measured with greater accuracy (for example, in the screw orientation the total width $r_{\mathrm{in}}+r_{\mathrm{ex}}$ of a double ribbon would be approximately eight times larger than the width of a dissociated dislocation).

(3) The displacement of the image with respect to the true position of the dislocations is, to a good approximation, the same for all three dislocations. r_{in} and r_{ex}, as directly measured from the micrographs, thus represent the true separation of the partials within the limits of the theory and no corrections have to be made.

In summary, because of the greater dissociation width, the insensitivity to internal stresses and the ease of image interpretation, it is expected that the evaluation of double ribbons will lead to more accurate values of both $\gamma_{\mathrm{in}} : \gamma_{\mathrm{ex}}$ and γ_{in} as compared to the values derived from single dissociated dislocations.

§ 3. Experimental details

The double ribbons discussed in this paper were formed by a disturbance of the dislocation network forming a low-angle twist boundary on {111} planes in Si. These grain boundaries were produced by welding two single crystals of Si with the required orientations, in a way similar to that described for gold by

Schober and Balluffi (1969), but differing in that the two single crystals were not thin foils when welded. Details of the welding technique and of experimental procedures are described by Föll and Ast (1978). The welded crystals were cut into specimens of a size suitable for TEM at an angle of $\sim 20°$ with respect to the boundary plane and subsequently thinned either chemically or by ion-milling.

There are three general features of boundaries prepared in this way.

(1) Low-angle boundaries consisting of fairly regular networks of primary dislocations with spacings up to ~ 50 nm (corresponding to a twist angle of $\sim 0{\cdot}4°$) can be produced.

(2) The boundaries generally contain precipitates (most likely amorphous SiO_2) which disturb the network.

(3) The network frequently responds to this disturbance by forming double ribbons which terminate at the precipitate in the way shown in fig. 1 (*a*). Double ribbons within the network are also observed.

The TEM observations were carried out in a Siemens Elmiskop 102 operated at 125 kV at electron-optical magnifications of $\times 100\,000$ or $\times 200\,000$. The magnification was directly calibrated by taking lattice-fringe images of $\{111\}$ planes at $\times 200\,000$. The objective current and thus the magnification were kept constant; focusing was done by vertical movements of the specimen. 220, 224, 111, and to a lesser extent 400 reflections were employed and the defects were imaged using the weak-beam technique (Cockayne, Ray and Whelan 1969).

§ 4. Experimental results

4.1. *General observations*

Typical examples of double ribbons imaged with different diffraction vectors are shown in figs. 2–4. Particular properties of the defects are seen best with particular diffraction vectors, e.g. 224 and 400 reflections give images with good contrast for all dislocations of the double ribbons and of the network and thus reveal best the geometry of the defects. Figure 2, as an example, demonstrates very clearly how the double ribbons are connected to the dislocation network. 220 reflections give images with the best contrast (fig. 3) and allow a Burgers vector analysis because one set of the three possible $a/6\langle 112\rangle$ partial dislocation Burgers vectors is completely out of contrast with one of the three 220 diffraction vectors in the $\{111\}$ planes of the defect. Finally using 111 reflections the stacking faults within the double ribbons (fig. 4) can be imaged. This obscures somewhat the contrast of the partial dislocations, but allows a simple analysis of the type of the stacking fault as shown below. The observed node networks consisted of screw nodes and most of the double ribbons lay within $\sim 10°$ of the screw orientation.

4.2. *Analysis of the type of the stacking fault*

The double ribbons discussed in this paper are intimately linked to the dislocation network of the small-angle grain boundary; the type of the stacking faults within a ribbon is therefore unambiguously given by the geometry of the

Fig. 2

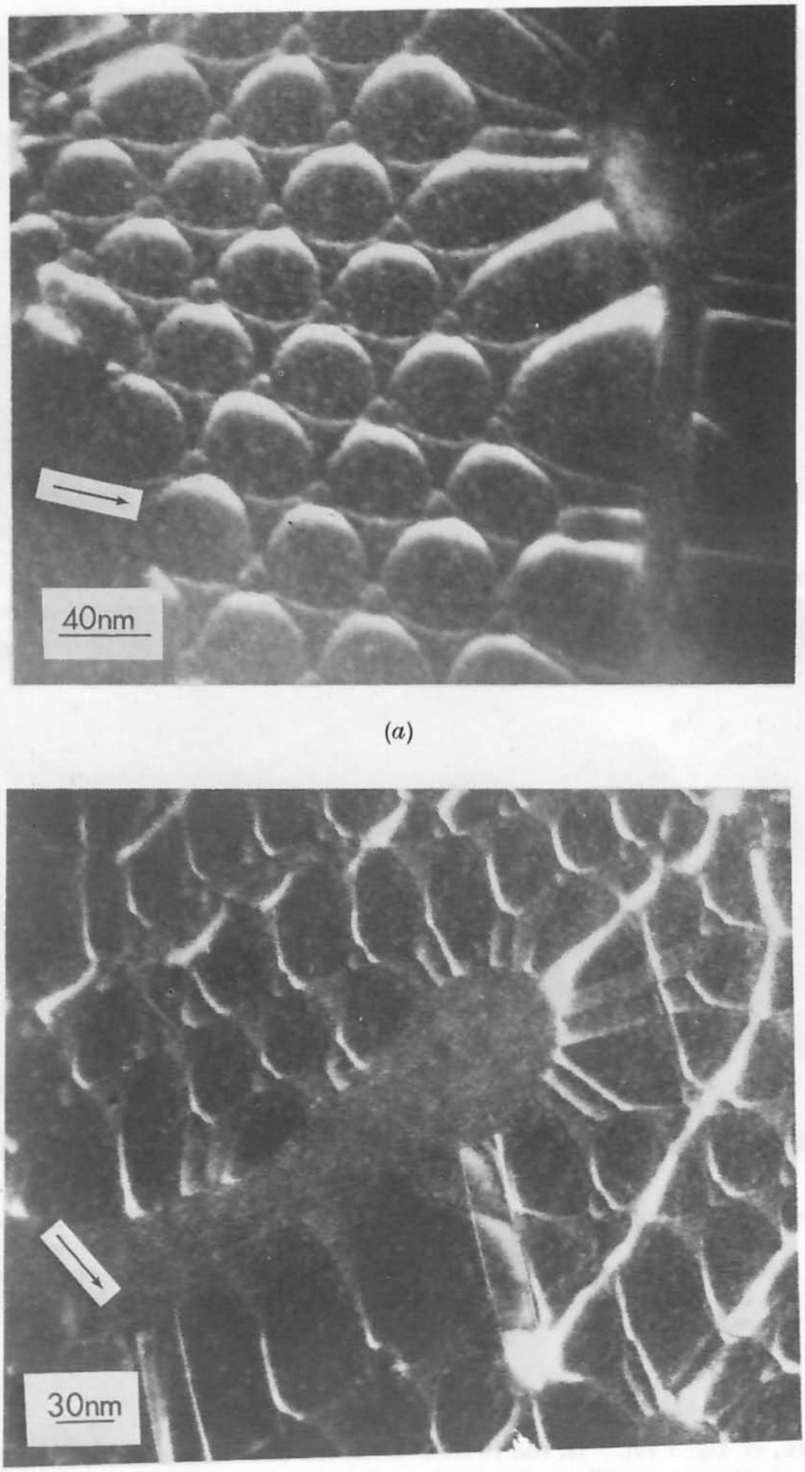

(*a*)

(*b*)

(*a*) Double ribbons close to the screw orientation imaged with a 224 reflection. (*b*) Double ribbons close to three different screw orientations imaged with a 400 reflection. The arrows indicate **g**.

Fig. 3

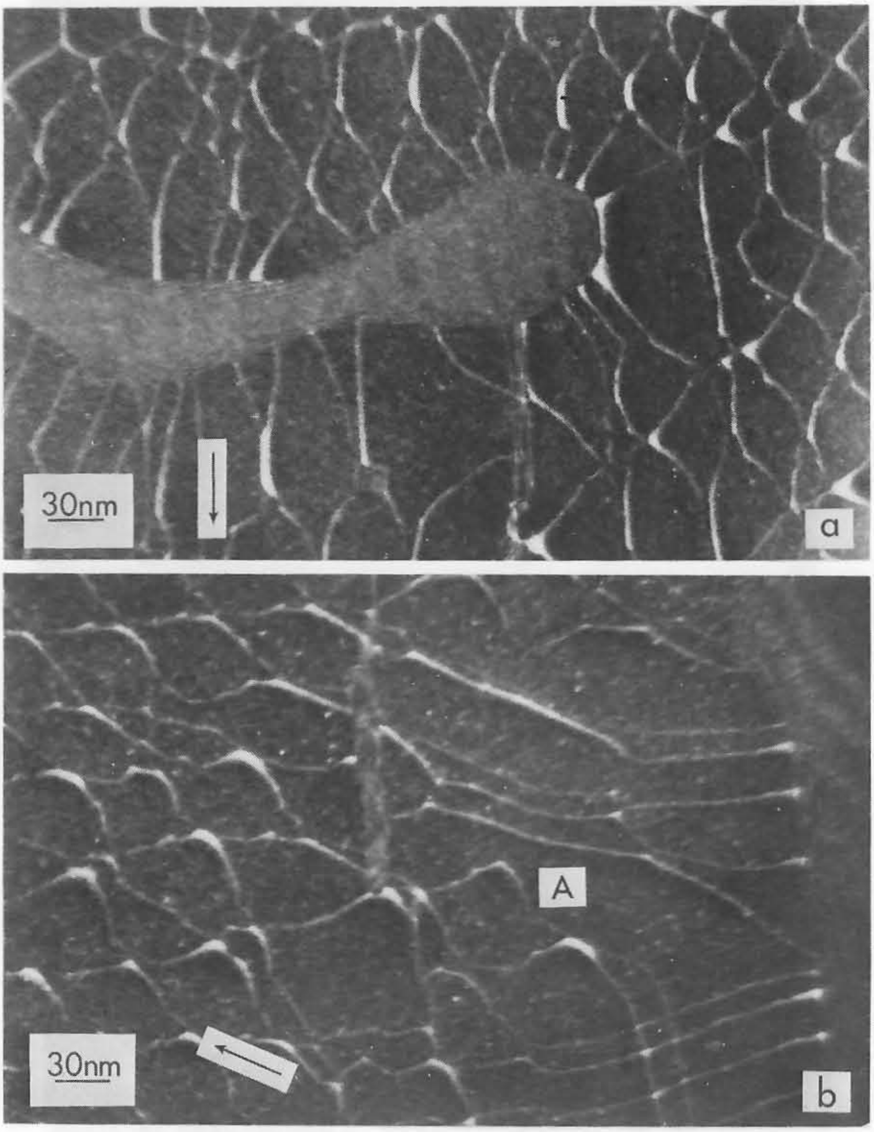

(*a*) Double ribbons of fig. 2 (*b*) imaged with a 220 reflection. Note that one of the double ribbons is completely out of contrast. (*b*) Double ribbon at A completely contained within the network. The arrows indicate the direction of the 2̄20 reflections used to form the weak-beam images, and the character varies from near screw to $\sim 30°$.

network, cf. fig. 1 (*a*). In the twist boundaries used in this study, the angle of misorientation was sufficiently small to give relatively well-defined dislocation node pairs similar to that discussed by Ray and Cockayne (1971). The nature of the stacking faults inside these dislocation nodes has been analysed independently by the authors, using variants of the inside–outside contrast technique. The results were identical: the stacking fault within the large nodes is of intrinsic type; the stacking fault within the small nodes is of extrinsic type. This result is consistent with the analysis of stacking faults in the nodes of a dislocation network in a Si–Ge interface (Cullis 1973) which appears to be similar to the network in the low-angle twist boundaries discussed here.

The analysis of Cullis (1973) was based on the observation that reversing the sign of a {111} diffraction vector shifts the contrast from the intrinsic to

Fig. 4

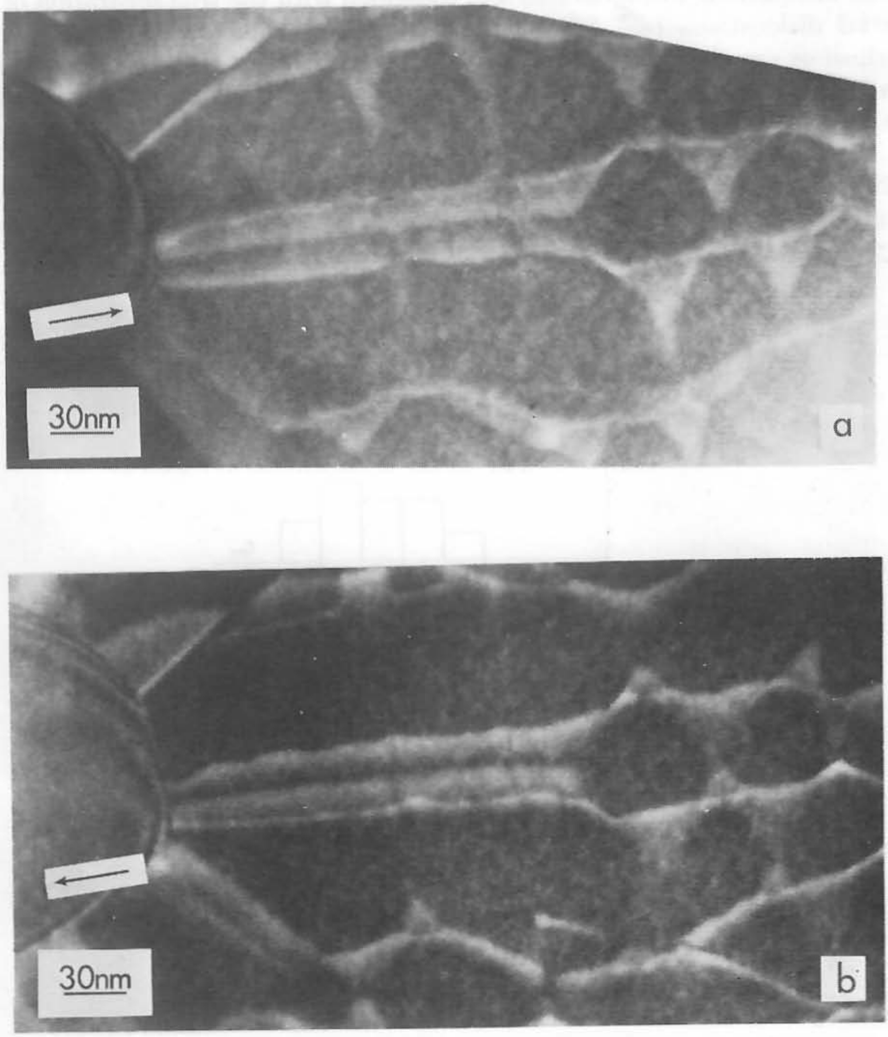

Double ribbon imaged with a 111 reflection. Note the change in contrast of the intrinsic node, the extrinsic ones, and the double ribbon, on reversing **g**. The nodes and the double ribbon are in the screw orientation.

of the stacking faults inside these dislocation nodes has been analysed independently by the authors, using variants of the inside–outside contrast technique. The results were identical: the stacking fault within the large nodes is of intrinsic type; the stacking fault within the small nodes is of extrinsic type. This result is consistent with the analysis of stacking faults in the nodes of a dislocation network in a Si–Ge interface (Cullis 1973) which appears to be similar to the network in the low-angle twist boundaries discussed here.

The analysis of Cullis (1973) was based on the observation that reversing the sign of a {111} diffraction vector shifts the contrast from the intrinsic to

Fig. 4

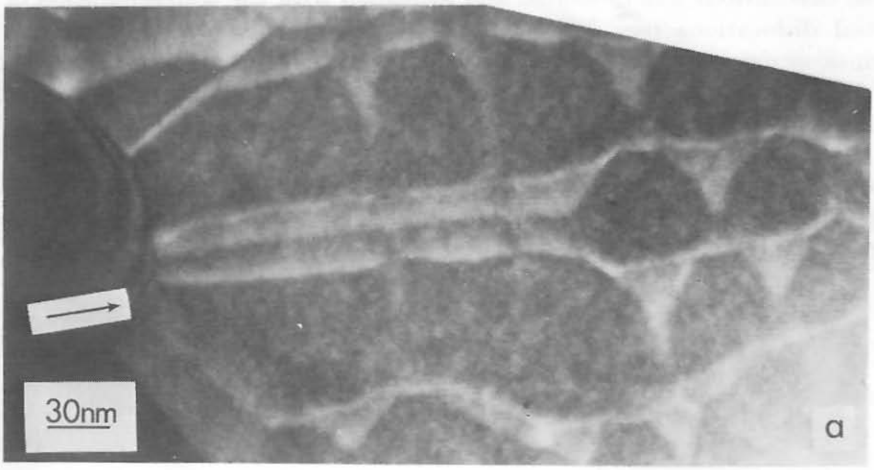

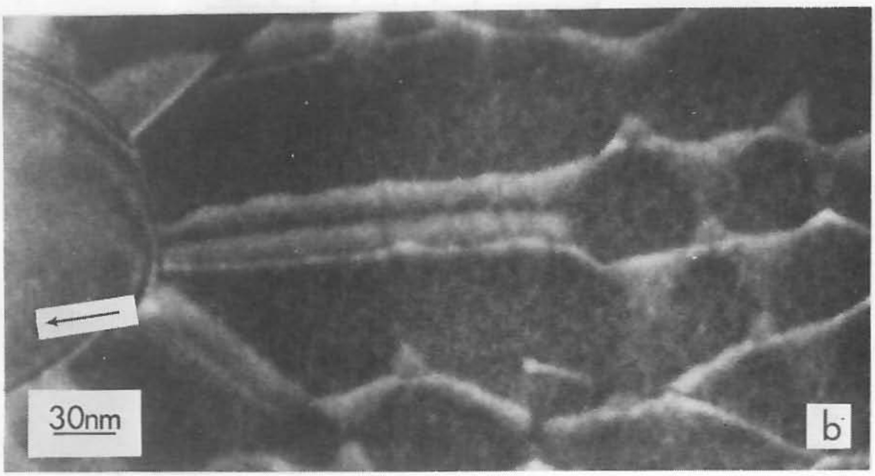

Double ribbon imaged with a 111 reflection. Note the change in contrast of the intrinsic node, the extrinsic ones, and the double ribbon, on reversing **g**. The nodes and the double ribbon are in the screw orientation.

the extrinsic stacking fault or vice versa. This effect offers a simple method for analysing stacking faults, but because the reason for this effect is not yet understood it must be calibrated before it can be applied to a particular type of sample.

In the present work the nature of the stacking faults and the sign of the Burgers vectors were obtained from the geometry of the network, from the inside–outside behaviour of the dislocation contrast, and from the fault-contrast reversal (calibrated here by the two other methods).

4.3. *Measurements of the distances between the partial dislocations in double ribbons*

Measurements have been made on 28 double ribbons lying within $\sim 10°$ of the screw orientation and which were sufficiently long for the partial dislocations to be parallel along the ribbon. The distance between the image peaks of the dislocations was measured and identified with the true separation of the partial dislocations (see § 2). The partial dislocations bounding either an intrinsic or extrinsic fault, or separating an intrinsic fault from an extrinsic one, can be physically different as indicated in fig. 1 (*b*), but this is not likely to significantly affect the measurements even under weak-beam conditions.

Micrographs taken with different reflections were evaluated separately; the $\sim 20°$ tilt of the $\{111\}$ plane containing the defect with respect to the image plane if a 111 reflection was used and the resulting slight image distortion was

Fig. 5

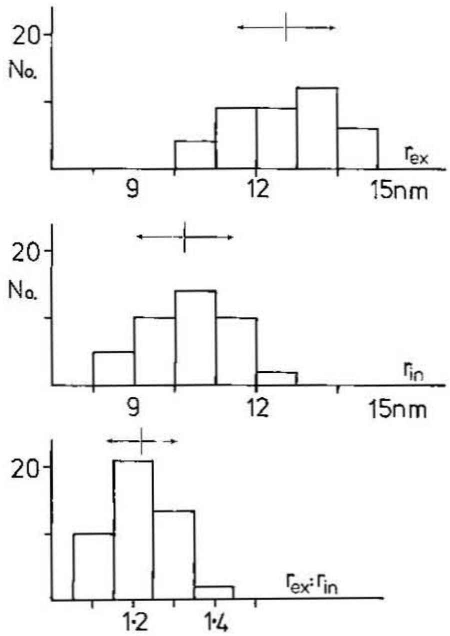

Histograms showing the distribution of r_{in}, r_{ex}, and $r_{in} : r_{ex}$. The mean values and the standard deviations are indicated and the double ribbons all lay within $\sim 10°$ of the screw orientation.

taken into account. The average distances between the dislocations bounding the intrinsic fault, r_{in}, or the extrinsic fault, r_{ex}, agreed well if measured with different reflections and were estimated to be (averaged over ~40 measurements, not including 111 reflections for γ_{in}, γ_{ex}; and ~50 measurements for $\gamma_{in}:\gamma_{ex}$)

$$r_{in}=10\cdot4 \text{ nm} \pm 12\%, \quad r_{ex}=12\cdot8 \text{ nm} \pm 12\% \quad \text{and} \quad r_{in}:r_{ex}=1\cdot23 \pm 8\%.$$

The corresponding stacking fault energies according to eqn. (1) are

$$\gamma_{in}=69 \pm 7 \text{ mJ m}^{-2}, \quad \gamma_{ex}=60 \pm 7 \text{ mJ m}^{-2} \quad \text{and} \quad \gamma_{in}:\gamma_{ex}=1\cdot15 \pm 0\cdot09.$$

The value for μ of $6\cdot36\times10^{10}$ N m^{-2} has been used as suggested by Aerts *et al.* (1962). This is the effective value for defects on the (111) plane and is only slightly below the Voigt average value of $6\cdot41\times10^{10}$ N m^{-2} (Hirth and Lothe 1968). The angle β is zero for the screw case and $|\mathbf{b}|$ is taken to be 0·222 nm.

It is important to note that, whereas both r_{in} and r_{ex} are susceptible to the usual systematic uncertainties, their ratio is *not* influenced by such errors (including the orientation): the ratio of the stacking fault energies is thus likely to be more accurate than the absolute values. This is reflected in the observed variations of $r_{in,ex}$ and $r_{in}:r_{ex}$, whereas r_{in} and r_{ex} show a standard deviation of ~12%, it is only ~8% for $r_{in}:r_{ex}$. Figure 5 shows a histogram of the observed values of r_{in}, r_{ex}, and $r_{in}:r_{ex}$.

4.4. *Isolated dislocations*

Impurities incorporated in the sample during the welding procedure at ~1200°C might influence the stacking fault energies. In order to be able to compare the present results with the results of other authors, relatively isolated dissociated screw dislocations lying in the boundary were investigated. Applying the standard procedure for estimating the stacking fault energy from the observation of single dislocations split into partials (Ray and Cockayne 1971), a value for $\gamma_{in}=60 \pm 10$ mJ m^{-2} was derived.

A further measurement was made on an isolated edge dislocation in the bulk material away from the boundary. Figure 6 shows weak-beam micrographs of this dislocation; two contrast peaks originating from the two partial dislocations are clearly visible. A value of $\gamma_{in}=60 \pm 10$ mJ m^{-2} was derived from the images obtained using the 220 reflections. 224 reflections were also used, giving image peaks from regions either inside or outside the defect as shown by Saldin, Cullis, Booker and Whelan (1974) and Gómez (1978) and allowing a simple analysis of the type of the stacking fault. The actual value of the separation of the partial dislocations *must* lie between the measured peak separations in the inside and outside images.

The measured image-peak separations, if taken as the true dissociation width of the partial dislocations, thus give an absolute upper and lower limit for the stacking fault energy, determined to be 70 mJ m^{-2} and 43 mJ m^{-2}.

§ 5. Discussion

5.1. *Possible error sources*

The double ribbons were formed during the welding procedure at a temperature of ~1200°C which is ~15% below the melting point of Si. At this

Fig. 6

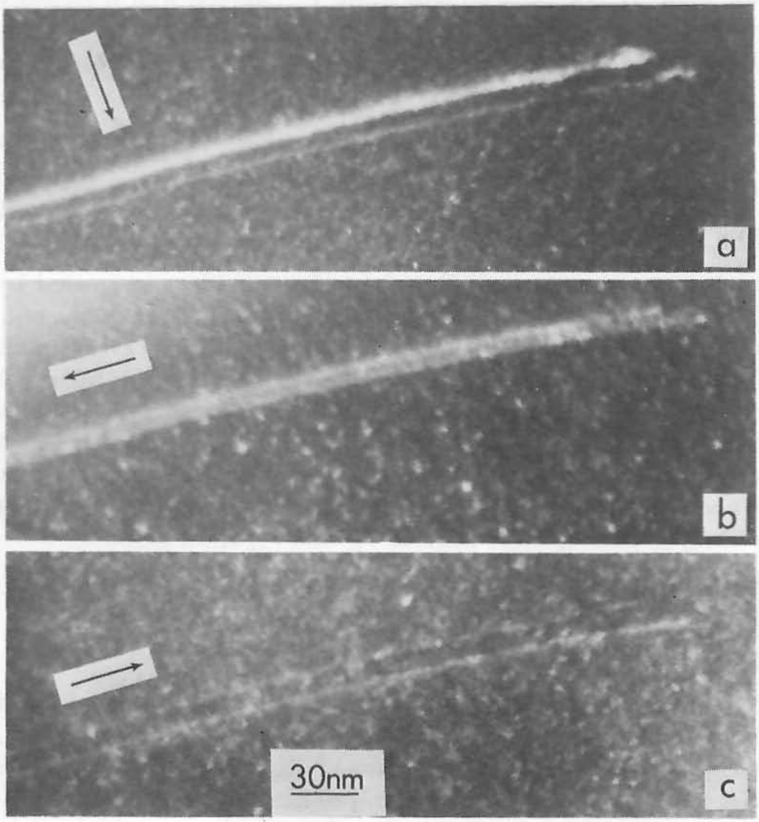

Weak-beam images of an edge dislocation in the bulk material. Note the inside-outside contrast behaviour with 224 reflections. The arrows indicate (*a*) $\mathbf{g}_{2\bar{2}0}$, (*b*) $\mathbf{g}_{\overline{224}}$, (*c*) $\mathbf{g}_{22\bar{4}}$.

temperature they were certainly in an equilibrium configuration. The specimens were cooled slowly in order to minimize residual stresses at room temperature. Dislocations in Si become immobile below $\sim 700°C$ (Alexander and Haasen 1968), and the dislocation structure observed at room temperature thus corresponds to the equilibrium structure at $\sim 700°C$ and is not changed during specimen preparation or under the influence of image forces due to free surfaces (Carter and Hazzledine 1977). This is directly confirmed by the observation that the dislocation network is not disturbed at its intersection with the specimen surface. The double ribbons observed at room temperature can thus be expected to represent their equilibrium structure for temperatures of approximately 700°C, and the stacking fault energy values given are thus values for this temperature region.

However, the nearby dislocations of the network may influence the width of double ribbons, although in practice the separation width of the partials was found to be fairly insensitive to the arrangement of nearby dislocations. Furthermore, double ribbons which were relatively isolated from the network gave values for γ_{in} and $\gamma_{in} : \gamma_{ex}$ in good agreement with those from double ribbons in closer contact to other dislocations. It is thus concluded that the results given above are not significantly influenced by the nearby network and that this effect is sufficiently accounted for by the experimental errors given by the scatter of the data.

For double ribbons ending at an amorphous precipitate no change in the separation width close to the interface was observed. Interface effects thus do not influence the measurements. This is further confirmed by the fact that double ribbons, completely contained within the dislocation network, show the same separation widths as double ribbons ending at an amorphous precipitate (see fig. 3 (*b*)).

Impurities may alter the stacking fault energy if incorporated in the fault. The presence of amorphous precipitates indicates that impurities are present in these samples, but that their influence on the stacking fault energy appears to be negligible for the following reason : (1) the stacking fault energies determined from isolated dislocations agree very well with the values in the literature for these defects (see the table) and (2) in the presence of a high density of dislocations, which can act as efficient traps for impurities, the incorporation of

γ_{in} (mJ m^{-2})	γ_{ex} (mJ m^{-2})	Defect	Reference
		Silicon	
51 ± 5	—	Isolated dislocations	Ray and Cockayne (1971)
50 ± 15	50 ± 15	Nodes (r) (*b*)	Ray and Cockayne (1971) (*a*, *f*)
71 ± 16	—	Nodes (w) (*b*)	Cullis (1973) (*f*)
58 ± 13	—	Nodes (r) (*b*)	Cullis (1973) (*f*)
70 ± 9	$\sim 0{\cdot}5\gamma_{in}$	Isolated screw dislocation	Gómez *et al.* (1975) (*c*)
76 ± 12	—	Faulted dipole	Spence and Kolar (1979)
69 ± 7	60 ± 7	Double ribbon	This paper
60 ± 10	—	Isolated dislocations	This paper
		Germanium	
60 ± 8	—	Isolated dislocations	Ray and Cockayne (1973)
67 ± 13	—	Isolated dislocations	Häussermann and Schaumburg (1973) (*d*)
60 ± 8	~ 30	Isolated dislocations	Gómez *et al.* (1975)
73 ± 9	—	Isolated edge dislocation	Packeiser and Haasen (1977) (*d*)
78 ± 16	—	Isolated screw dislocation	Packeiser and Haasen (1977) (*d*, *e*)
100 ± 10	$\lesssim \gamma_{in}$	Dislocation in grain boundary	Bourret and Dessaux (1979)

(*a*) γ_{ex} was stated to be ‘ of the same order of magnitude ’ as γ_{in}.
(*b*) w is the radius of the inscribed circle and r is the radius of curvature of the partials at the node.
(*c*) The value for γ_{in} is deduced from the data points given in this paper in addition to the original points of Ray and Cockayne (1971).
(*d*) These values were deduced from determinations of the distance between partials reported in these papers using the curves of Gómez *et al.* (1975).
(*e*) The value given assumes a width of between 2 nm and 3 nm.
(*f*) The values were deduced by setting $\mu = c_{44} = 7{\cdot}9 \times 10^{10}$ Nm^{-2}. For comparison with the values deduced in the present study they should be multiplied by a factor 0·8.

impurity atoms in the stacking fault is only likely if it results in a lowering of the stacking fault energy. Since the value for the intrinsic stacking fault energy reported here is higher than the values reported elsewhere, an influence of impurities on the defects studied would be to increase the discrepancy.

Whenever possible, focusing was done by moving the specimen rather than changing the objective current, thus achieving constant magnification.

Finally, it should be mentioned that defects with the appearance of double ribbons can be formed by partially overlapping two dissociated dislocations on non-adjacent {111} planes. This possibility can be safely excluded in this case since the double ribbons are part of a dislocation network. In addition, pseudo-double ribbons would be much smaller than the ones observed here (Amelinckx 1977, Carter 1979).

In conclusion, the error bars for the values given here are believed to be adequately represented by the standard deviation values of $\sim 12\%$ for $\gamma_{\mathrm{in,ex}}$ and $\sim 8\%$ for $\gamma_{\mathrm{in}} : \gamma_{\mathrm{ex}}$.

5.2. *The ratio of the stacking fault energies*

The ratio $\gamma_{\mathrm{in}} : \gamma_{\mathrm{ex}}$ of $1{\cdot}15 \pm 0{\cdot}09$ determined in this study is thought to be more reliable than that determined from separate defects containing intrinsic or extrinsic faults.

The only other direct estimate of $\gamma_{\mathrm{in}} : \gamma_{\mathrm{ex}}$ in silicon was made by Gómez *et al.* (1975) who observed that the dissociation width of dislocations close to the screw orientation was particularly large if the stacking fault was of the extrinsic type. This observation was interpreted as showing that the extrinsic stacking fault energy is approximately half that of the intrinsic fault. In view of the present results it is clear that this explanation cannot be valid.

It is possible that the different core structures of the bounding partials are responsible for this anomaly, either by affecting the elastic interactions between the partial dislocations, which would be most likely to occur for isolated dislocations near the screw orientation, or by giving different Coulomb repulsion terms (Hirsch 1978) compared to the intrinsic stacking fault case.

Bourret and Dessaux (1979) have recently obtained a value $\gamma_{\mathrm{in}} : \gamma_{\mathrm{ex}} \sim 1$ and $\gamma_{\mathrm{in}} \sim 100$ mJ m^{-2} from lattice-fringe images of dislocations in a low-angle tilt boundary in Ge. While the reliability of this method requires further study, the results do support the present value for the ratio in Si.

5.3. *The absolute value of γ*

Values for $\gamma_{\mathrm{in,ex}}$ derived from measurements using either the weak-beam technique or lattice-fringe images are given in the table for Si (and for comparison for Ge).

Because of the large size of the defects and the simplicity of the interpretation it is suggested that the values for γ_{in} and especially that for γ_{ex} is best given by the double-ribbon result. The value for γ_{in} of 69 ± 7 mJ m^{-2} is in excellent agreement with the result deduced from recent measurements of Gómez *et al.* (1975) and suggests that the earlier value obtained by Ray and Cockayne (1971) is a little too low. Isolated dislocations both in the boundary and in the bulk material did however also give a somewhat lower value in the present study. It is possible that this is partially due to the type of defect used to make the determination of γ as suggested in § 5.2. For example the values deduced from extended nodes give a consistently lower value for γ_{in} if $\mu = 6{\cdot}36 \times 10^{10}$ N m^{-2} is used.

It has recently been suggested (Hirsch 1978) that charge effects may play a significant role for the separation width of partial dislocations in semiconductors. Because the partial dislocations have pure screw character it appears that this effect would not significantly influence the double ribbon results, but the influence of an additional repulsive force between partial dislocations arising from charge effects certainly requires further consideration.

§ 6. Conclusions

The intrinsic and extrinsic stacking fault energies of silicon have been determined from observations on double ribbons near the screw orientation which were formed in a low-angle twist boundaries obtained by welding The values found were $\gamma_{\mathrm{in}} = 69 \pm 7$ mJ m^{-2}, $\gamma_{\mathrm{ex}} = 60 \pm 7$ mJ m^{-2} and $\gamma_{\mathrm{in}} : \gamma_{\mathrm{ex}} = 1{\cdot}15 \pm 0{\cdot}09$. The intrsinsic stacking fault energy was also determined from relatively isolated screw dislocations in the boundary and isolated edge dislocations in the bulk ; both give a value of 60 ± 10 mJ m^{-2} using the conventional interpretation based on continuum elasticity. It is suggested that the early measurements on isolated dislocations gave a value for the stacking fault energy which was a little too low. There is evidence that the type of defect used to determine the value for the stacking fault energy may influence the value derived and it is suggested that the large size of the double ribbons studied here, together with their pure screw character, make the values given above the most reliable.

Acknowledgments

This work was supported by DOE under contract No. EY–76–S–02–2899 and by the National Science Foundation through the Materials Science Center at Cornell University. The authors would like to thank Dr. D. J. H. Cockayne and Professor D. Ast for carefully criticizing the manuscript, and Dr. B. O. Kolbesen from the Siemens AG for kindly supplying the silicon used for the present study.

References

Aerts, E., Delavignette, P., Siems, R., and Amelinckx, S., 1962, *J. appl. Phys.*, **33,** 3078.

Alexander, H., and Haasen, P., 1968, *Solid St. Phys.*, **22,** 27.

Amelinckx, S., 1977, *Dislocations in Solids*, Vol. 2, edited by F. R. Nabarro (North Holland).

Blanc, J., 1975, *Phil. Mag.*, **32,** 1023.

Booker, G. R., and Brown, L. M., 1965, *Phil. Mag.*, **11,** 1315.

Bourret, A., and Desseaux, J., 1979, *Phil. Mag.* A, **39,** 405, 419.

Carter, C. B., 1979 (submitted for publication).

Carter, C. B., and Hazzledine, P. M., 1977 (unpublished research).

Cockayne, D. J. H., Ray, I. L. F., and Whelan, M. J., 1969, *Phil. Mag.*, **20,** 1265.

Cullis, A. G., 1973, *J. Microsc.*, **98,** 191.

Delavignette, P., and Amelinckx, S., 1961, *J. nucl. Mater.*, **5,** 17.

Föll, H., and Ast, D., 1978, *Proceedings of the Ninth International Congress on Electron Microscopy, Toronto*, Vol. 1 (Microscopical Society of Canada), p. 428.
Gallagher, P. C. J., 1966, *Phys. Stat. Sol.*, **16**, 95.
Gómez, A. M., 1978, *Phil. Mag.* A, **37**, 435.
Gómez, A., Cockayne, D. J. H., Hirsch, P. B., and Vitek, V., 1975, *Phil. Mag.*, **31**, 105.
Haasen, P., and Schröter, W., 1970, *Fundamental Aspects of Dislocation Theory*, edited by J. A. Simmons, R. de Wit and R. Bullough. Special Publication 317, 2 (U.S. National Bureau of Standards), p. 1231.
Häussermann, F., and Schaumberg, H., 1973, *Phil. Mag.*, **27**, 745.
Hirsch, P. B., 1978, *Proceedings of the Ninth International Congress on Electron Microscopy, Toronto*, Vol. III (Microscopical Society of Canada), p. 369.
Hirth, J. P., and Lothe, J., 1968, *Theory of Dislocations* (New York : McGraw-Hill), pp. 356 ff.
Labusch, R., and Schröter, W., 1975, *Lattice Defects in Semiconductors*, Conference Series No. 23 (Institute of Physics), p. 56.
Packeiser, G., and Haasen, P., 1977, *Phil. Mag.*, **35**, 821.
Ray, I. L. F., and Cockayne, D. J. H., 1971, *Proc. R. Soc.* A, **325**, 543 ; 1973, *J. Microsc.*, **98**, 170.
Ruff, A. W., and Ives, L. K., 1969, *Acta metall.*, **17**, 1045.
Saldin, D. K., Cullis, A. G., Booker, G. R., and Whelan, M. J., 1974, *Proceedings of the Eighth International Congress on Electron Microscopy, Canberra*, Vol. 1 (Microscopical Society of Australia), p. 458.
Schober, T., and Balluffi, R. W., 1969, *Phil. Mag.*, **20**, 511.
Spence, J. C. H., and Kolar, H., 1979, *Phil. Mag.*, **39**, 59.
Wessel, K., and Alexander, H., 1977, *Phil. Mag.*, **35**, 1523.